International Journal of Scientific Engineering and Applied Science (IJSEAS) – Volume-7, Issue-9, September 2021
ISSN: 2395-3470
www.ijseas.com

Synthesis of SnS Nanoparticles for Next Generation Photovoltaic Applications

A.P. Sunitha[1], K. Nayana[2], M.S. Arya[3], S. B. Rakesh Chandran[4]

[1]Department of Physics, Government Victoria College, Palakkad, Kerala-678001,University of Calicut

[2]NSS College, Ottapalam, Palakkad, Kerala-, University of Calicut

[3]Sree Vivekananda Padana Kendra Arts and Science College, Malappuram, Kerala-679331, University of Calicut

[4]Department of Physics, Sanathana Dharma College, Alappuzha, Kerala-688003,University of Kerala

E-mail: sunithaganesh@gvc.ac.in

Abstract

Tin mono sulfide (SnS) is one of the promising materials for the development of photochemical cells, photo detectors, solid-state batteries, sensors, capacitors etc. Herein, we synthesized SnS nanoparticles by wet chemical method for next generation eco-friendly solar cells and other photovoltaic applications. It is the method which involves growing of nanoparticles in a liquid medium having different reactants. Tin chloride and Sodium sulfide were taken as the reactants. These SnS nanoparticles were characterized by spectroscopic, microscopic, and scattering techniques. From the absorption spectroscopy the prepared SnS nanoparticles have an average direct bandgap of 1.89 eV and indirect band gap of 1.24 eV which are suitable to act as an active layer for solar cells. Blue shift of bandgap indicates the phonon confinement effect and nanostructure of synthesized SnS. Moreover, from the Transmission Electron Microscopic images the uniform size formation of SnS nanoparticles with a size in range 2-5 nm that is acceptable for the gas sensing were confirmed. In the XRD analysis, the sharp and strong diffraction peaks indicates that the nanoparticles were well crystallized and were indexed to pure orthorhombic phase of SnS. Calculated lattice parameters and d spacing confirm the crystalline structure. Raman spectra also confirm the crystalline structure of SnS. The average particle size of SnS was characterized by Dynamic Light Scattering (DLS) measurement. The poly crystalline nature of SnS was found by SAED pattern. Thus, the synthetic methodology opens up the possibility of generating low-cost photovoltaic devices based on SnS film as an active layer through a scalable chemical pathway.

Introduction

SnS possess wide potential applications. In research, because of structural, chemical, physical and luminescence properties of SnS the semiconductor nanocrystals are widely studied [1]. SnS nanoparticles show great promise in the field of photoelectric [2-3] and thermoelectric [4-5]

devices [6]. By using solvothermal [7-8], and hydrothermal [9], successive ionic layer adsorption and reaction [10-11], wet chemical synthesis [12-13], pulsed laser deposition [14], thermal evaporation [15], physical vapor deposition [16], electrochemical [17] methods etc., SnS nanostructures with different morphologies such as nanosheets, nanorods, nanowires and nanoflowers can be synthesized.

SnS is used in perovskite [7,18] and quantum dot sensitized [10,19-21] solar cells, photodetectors, solid-state batteries [8,16], capacitors [17,22], Sensors [23-24], holographic recording medium [25-26] and an efficient visible light driven photocatalytic material [27] due to its promising physical and chemical properties. Hence, SnS finds extensive interest in many fields of science and technology [28]. Among the semiconductors, tin sulfide is an important 4-6 group layered semiconductor with an optical direct bandgap of about 1.3 eV and indirect band gap of about 1 eV, which is a little smaller than that of CdS [7,22,29]. Such a bandgap of SnS make it a potential candidate for efficient solar cell. In this view CdS can be replaced by SnS, which can satisfy the requirements for photo conducting applications [30]. SnS is an efficient semiconductor material with Sn and S atoms are covalently bonded tightly and having orthorhombic crystal structure and higher absorption coefficient [25]. It is a good candidate for non-toxic and non-expensive photo absorber material [16, 31-32]. SnS possess uniqueness in crystal structure and can be zero-dimensional semiconductor nanostructure which can be varied from p-type to n-type by controlling the concentration of tin atoms [22, 28, 33]. By adding different dopants it's conductivity control can be possible [5, 17, 34]. SnS has narrow band gap which is optically active in NIR and IR region [9, 35]. High carrier concentration and high absorbance in visible light and IR radiation make SnS as a good candidate in solar cells and thermoelectric applications [4-5].The good stoichiometry properties and the chain like structure of SnS increases the sensitivity of gas sensing [23-24]. These applications insisted to research for a simple and convenient method of synthesis of SnS nanoparticles with narrow sizes and wide optical properties [36].

Experimental

Materials: Tin chloride ($SnCl_2$-$2H_2O$), Sodium sulfide (Na_2S), Isopropyl alcohol (IPA) and deionized water were used as precursors. The SnS nanoparticles were synthesized by wet chemical method by the following fundamental steps. The precursor materials were completely dissolved in deionized water and mixed in a flask and stirred it till completely mixed. The precipitate formed was further centrifuged and washed several times with IPA (Isopropyl

alcohol) and deionized water respectively to remove impurities. The final product was dried to get the nanoparticles.

Tin chloride ($SnCl_2$-$2H_2O$) and Sodium sulfide (Na_2S) were taken as tin and sulfur precursors respectively. 0.5 molar solutions of$SnCl_2$-$2H_2O$ (3.792g in 40 ml deionized water) and Na_2S (1.56g in 40 ml deionized water)were prepared. Sodium sulfide solution was added drop wise in to the tin chloride solution by continuously stirred. The turning of colorless tin chloride solution in to the dark brown indicates the formation of SnS nanoparticles. The solution was stirred continuously with a magnetic stirrer for 2 hours. Then the stirred solution was further washed at 2000 rpm for 5 minutes with IPA and deionized water. The precipitate thus formed heated at 80°C in the oven for 2 hours. Figure 1 shows the SnS nanoparticles that formed as the final product of the synthesis.

Results and discussions

The synthesized SnS nanoparticles were quantitatively analyzed and characterized in terms of their morphological, structural and optical properties. At ambient temperature by simple chemical method the SnS nanoparticles were synthesized. The structural characterization was done by XRD (Cu-K_α with wavelength 1.5405 A^0), TEM and DLS (Nano Particle Analyzer SZ–100-Horiba) techniques respectively. The optical studies were carried out by UV-VIS-NIR spectroscopy (Jasco V–570 UV/VIS/ NIR Spectrophotometer). Raman spectroscopic study was done by Jobin Yvon Lab RAM HR Spectrophotometer with Ar ion laser, 514.5 nm.

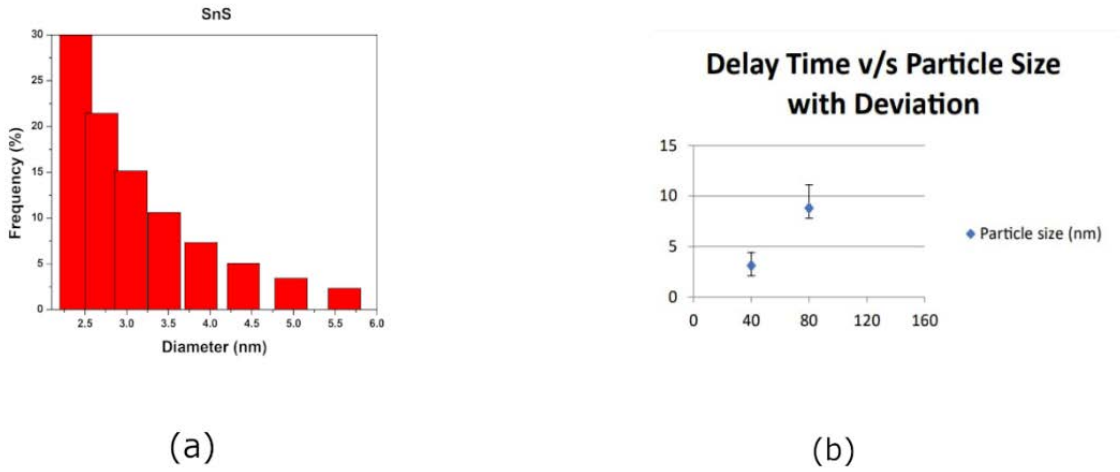

Figure 1(a). Histogram showing the size distribution of SnS nanoparticles. (b) Graph showing variation b/t Delay time and SD with Particle size

DLS technique gives the distribution of particles and corresponding particle size [37]. The histograms of size distribution of SnS nanoparticles are shown in Figure 1(a). The particle size of the obtained SnS is in the range of 2-5 nm which shows the particles are in nanometric range. As the sample contains particles with multiple sizes (according to TEM images) DLS measurements were done for 3 different gate delay times and the mean size with standard deviation is plotted. Particle size estimation at 40 ns, 80 ns & 160 ns gate delay time was carried out with the prepared sample.

Figure 2 shows the powder XRD pattern of tin sulfide nanoparticles. In XRD pattern, a prominent diffraction peak was observed at glancing angle 2θ, 31.56°, which corresponds to the reflection plane (1 1 1) and the other medium intensity peaks at 2θ, 27.5° and 45.5° which corresponds to the (0 2 1) and (0 0 2) reflection planes respectively [7, 9, 21, 38]. All the diffraction peaks were indexed to pure orthorhombic phase of SnS (JCPDS card no. 00-039-0354) [7, 9, 11, 21, 38]. It is due to the clustering of particles in the powdered sample and hence it is used for phase identification [7, 21, 38]. The sharp and strong diffraction peaks indicates that the nanoparticles were well crystallized. Since no other impurity peaks were observed, the phase purity is confirmed from the powder XRD. Interplanar distances can be calculated using the equation (1) and results are tabulated in table-1. Lattice parameters are calculated by the equation (2) [39-40] with a= 4.272 A^o, b= 11.256 A^o and c= 3.98 A^o. The values are in well match with the lattice parameters of orthorhombic structure of SnS [9, 15, 21, 39, 41]. Average crystallite size (D) is estimated by the equation (3) as 50.6 nm. β is the full width at half maximum of the prominent peak (1 1 1) in radian and λ is the wavelength of light (Cu Kα) 1.54 A^o used in XRD. K is 0.9.

$$2d\sin\Theta = \lambda \quad (1)$$

$$1/d^2 = h^2/a^2 + k^2/b^2 + l^2/c^2 \quad (2)$$

$$D = K\lambda/\beta\cos\Theta \quad (3)$$

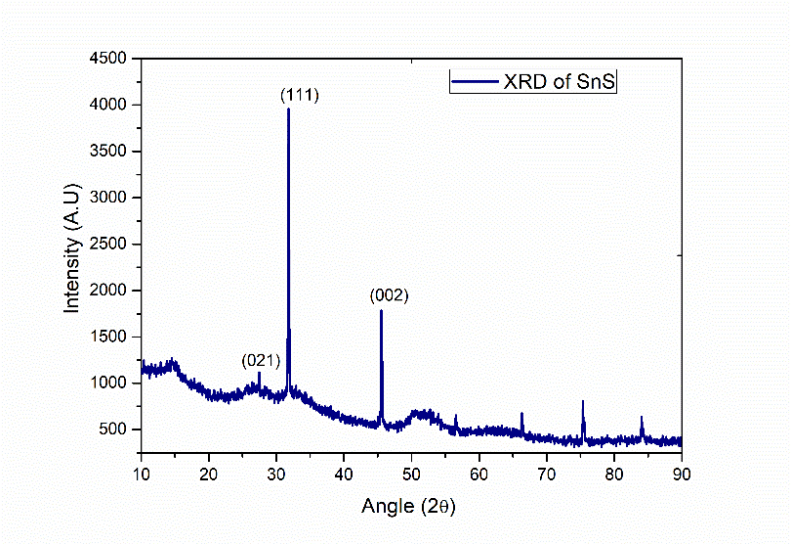

Figure 2. XRD pattern of synthesized SnS nanoparticles

(HKL)	2Θ (DEGREE)	INTERPLANAR DISTANCE (A^O)	INTERPLANAR DISTANCE FROM JCPDS [11]
021	27.4	3.25	3.38
111	31.75	2.82	2.85
002	45.49	1.99	-

Table-1. Interplanar distance from XRD

The particle size distribution measured by the TEM imaging is shown in Figure 3(a-b). Crystalline structure with interplanar distance of 2.27 A^o agrees with the d space got from XRD and JCPDS data. Li. Y et al., Tripathi A.M et al., Han J et al., Li. H et al. and Sohila. S et al., have reported 2.8 A^o, 2.95 A^o, 2.8 A^o, 2.84 A^o and 3.25 A^o, as interplanar distance from TEM images respectively [7-8, 18, 20, 38]. The images confirmed the formation of very small spherical SnS nanoparticles and most of them were clustered together in the form of poly dispersive nanoclusters [42]. The prepared samples of SnS nanoparticles in high resolution TEM indicates the presence of nanoparticle agglomeration of size 2-100 nm, with individual particles of average size between 2-5 nm. From these figures it is evident that the SnS nanostructures are clustered among themselves. This kind of agglomeration is quite common in SnS nanopowders [38].

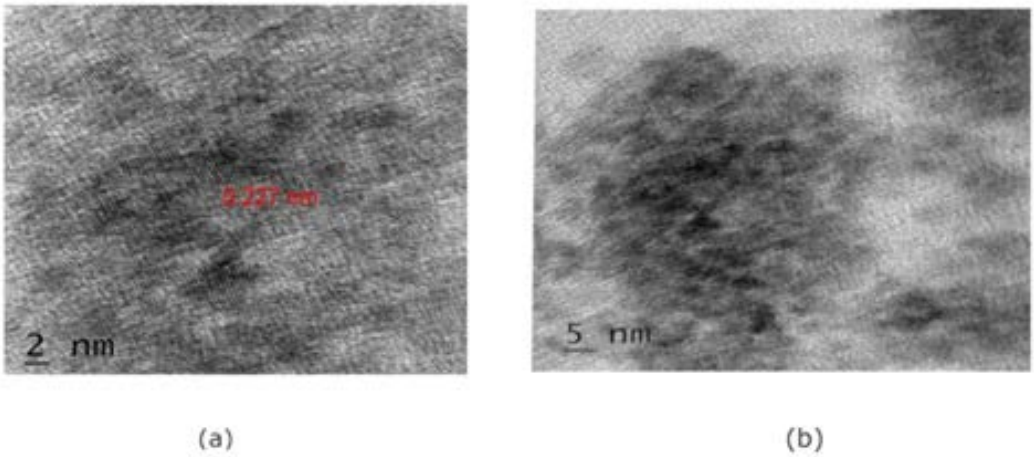

Figure 3(a-b): TEM images of prepared nanoparticles

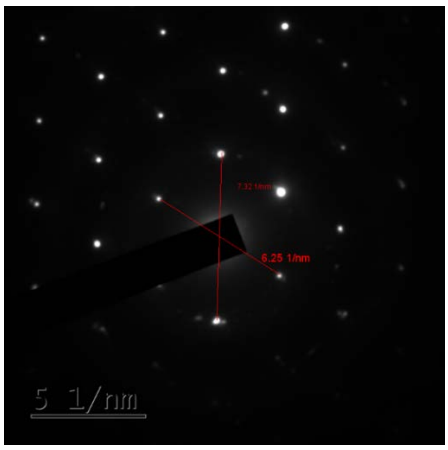

Figure 4. SAED image of obtained SnS nanoparticles

Figure 4 shows the selected area electron diffraction (SAED) image taken from the synthesized nanostructure. The figure shows dots clearly the formation of polycrystalline nature of nanoparticles. Similar results in various research works confirm the polycrystallite behavior [8, 16, 38]. Interplanar distance (d) calculated by the equation (4), are 3.2 A^o and 2.73 A^o where r is the radius between bright spots. These are in good match with interplanar distances tabulated in table-1. K. G. Deepa et al. reported interplanar distance of 2.86A^o for the plane (111) [21]. The SAED results remains in a good agreement with the XRD data.

$$d = 1/r \qquad (4)$$

The absorption spectrum of SnS shows the absorption begins near at 800 nm and reaches maximum at 368 nm making the SnS material extremely useful as absorber layer [16-17, 43]. Figure 5(a) represents the variation of optical absorbance with the wavelength of prepared SnS nanoparticles. It is clear that the nanoparticles have a wide absorption range from the NIR to the

UV, which means it is good for absorption of sunlight [9, 35]. The direct and indirect bandgap of prepared SnS nanoparticles were calculated using equation (5). Direct band gap of 1.89 eV and indirect band gap of 1.24 eV indicate the blue shifting of bang gap energies from bulk SnS. Sohila et al. reported a direct band gap of 1.78 eV and indirect band gap of 1.2 eV [38]. Similarly, W. Guo et al. reported 2.4 eV and 1.6 eV respectively for direct and indirect band gaps [19]. Both of them reported the factors affecting band gap energy include the size quantization in SnS crystal [19, 38]. Sebastian et al. reported a direct band gap of 1.68 eV [39], Tripathi A.M et al reported an indirect band gap of 1.2eV [8], and Xu Y et al reported an indirect band gap of 1.1 eV [35]. Here n=1/2 for direct band gap and n=2 for indirect band gap [8, 17, 22, 39, 44]. Corresponding Tauc plots are shown in Figure 5(b) and 5(c). The band gap increases as the particle size decreases in semiconductor nanoparticles. The figure shows that the absorption had a peak corresponding to wavelength around 300 nm to 500 nm and the peak formed was not sharp. It is due to the large size distribution, different particle morphologies and impurities attached to particles surfaces, the peaks were broadened. The absorption reduces rapidly with increase in wavelength and it becomes very small or zero at a wavelength range above 800 nm [35]. Refractive index (n) of as synthesized SnS quantum dots can be roughly calculated using the relation (6). By substituting direct band gap energy (E_g) of 1.89 eV, refractive index is 2.75 [44].

$$\alpha h\nu = A\,(h\nu - E_b)^n \qquad (5)$$

$$n = (\,95/E_g)^{0.25} \qquad (6)$$

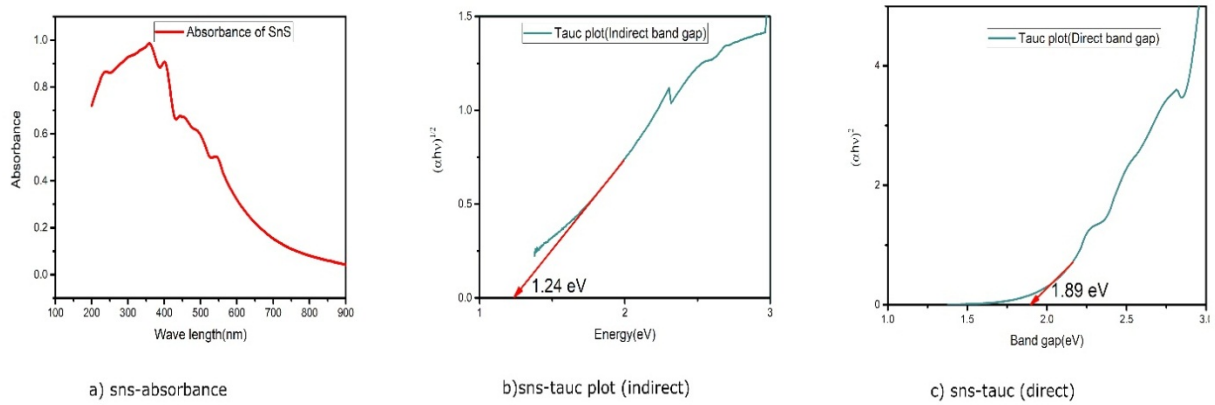

Figure 5. (a)Absorption spectrum of SnS nanoparticles. (b) Tauc plot for indirect band gap. (c) Tauc plot for direct band gap

Raman spectra of SnS quantum dots again confirm the presence of pure crystalline structure of it. Excitation wavelength used is 514.5 nm. Peaks at 104 cm^{-1} and 180.5 cm^{-1} are representing A_g and B_{3g} modes of SnS [9, 16, 38]. For SnS among 21 vibrational modes 12 are Raman active [9, 16, 38, 41, 45-46]. S. Sohila et al. and Priyal Jain et al. reported that broadening of Raman peaks is due to the phonon confinement effect [15, 38]. H. C. Choi et al. and Priyal et al. also reported that shift in peak depend on grain size [15, 47]. C. Y. Xu et al. explained the broadening of Raman peaks with the help of Heisenberg's uncertainty relation [48]. In nanoscale, since the grain size reduces, the phonon positions are confined to the size of the particle. Then the phonon momentum increases which results in the broadening of Raman peaks. The broad peaks in figure 6 reveal that the size of synthesized SnS is in quantum dot range.

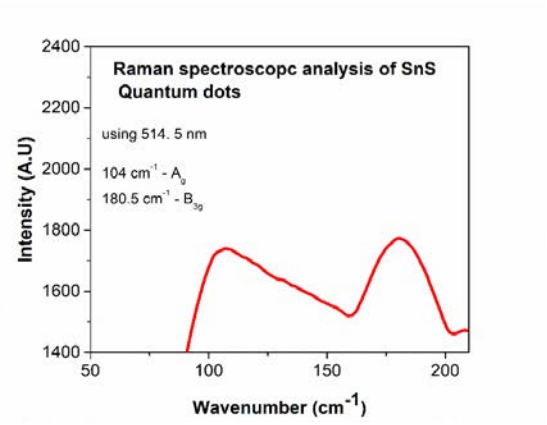

Figure 6. Raman spectra of SnS quantum dots

Conclusion

The SnS nanoparticles were synthesised at ambient temperature by simple chemical method. The obtained nanoparticles were quantitatively analyzed and characterized in terms of their morphological, structural and optical properties. The structural characterization was done by XRD,TEM and DLS techniques respectively. The optical studies were carried out by UV-VIS-NIR spectroscopy. The XRD pattern showed the orthorhombic phase of SnS nanoparticles. Interplanar distances and crystallite size are calculated from XRD. The average particle size 2-5 nm and interplanar distance were confirmed by DLS analysis and TEM imaging respectively. The particle size range is acceptable for gas sensing. The SAED revealed the crystalline structure and interplanar distance of the synthesized nanostructures. Also, the absorption spectrum shows that prepared nanoparticles have a wide absorption range. The band gap energies in the range of near infrared and visible light make the nanostructures suitable to act as an active layer for solar cell. Raman spectrum confirms the pure crystal nature of SnS and its quantum dot behavior. The

quality of synthesized SnS nanostructures can also be easily turned by changing the growth or deposition conditions of the associated technique.

Very simple, non- expensive and eco-friendly procedure was used to synthesis SnS nanoparticles successfully at normal laboratory conditions with a bandgap which is favourable for using SnS as a semiconductor and photovoltaic devices.

Acknowledgement

We are very thankful to Dr. K J Saji, International School of Photonics, CUSAT,Kochin-22 for the support and providing help for the characterization of the sample.

Reference

1. Chandan Rana, Swades Ranjan Bera, Satyajit Saha, Growth of SnS nanoparticles and it's ability as ethanol gas sensor, journal of Materials Science: Materials in Electronics,https://doi.org/10.1007/s10854-018-0473-3.
2. A.tanusevski.Optical and photoelectric properties of SnS thin films prepared by chemical bath deposition.Semicond. Sci. Technol. 18 (2003) 501–505
3. Patel M, Kim HS, Kim J. Wafer-scale production of vertical SnS multilayers for high-performing photoelectric devices. *Nanoscale*. 2017;9(41):15804-15812. doi:10.1039/c7nr03370b
4. Azizian-Kalandaragh Y, Khodayari A, Zeng Z, Garoufalis CS, Baskoutas S, Gontard LC. Strong quantum confinement effects in SnS nanocrystals produced by ultrasound-assisted method. *J Nanoparticle Res*. 2013;15(1). doi:10.1007/s11051-012-1388-1
5. Zhou B, Li S, Li W, et al. Thermoelectric properties of SnS with na-doping. *ACS Appl Mater Interfaces*. 2017;9(39):34033-34041. doi:10.1021/acsami.7b08770
6. Xu Y, Al-Salim N, Tilley RD. Synthesis and Size Dependent Reflectance Study of Water Soluble SnS Nanoparticles. *Nanomaterials*. 2012;2(1):54-64. doi:10.3390/nano2010054
7. Li Y, Wang Z, Ren D, et al. SnS Quantum Dots as Hole Transporter of Perovskite Solar Cells. *ACS Appl Energy Mater*. 2019;2(5):3822-3829. doi:10.1021/acsaem.9b00510
8. Tripathi AM, Mitra S. Tin sulfide (SnS) nanorods: Structural, optical and lithium storage property study. *RSC Adv*. 2014;4(20):10358-10366. doi:10.1039/c3ra46308g
9. Ali S, Wang F, Zafar S, Iqbal T. Hydrothermal Synthesis, Characterization and Raman Vibrations of Chalcogenide SnS Nanorods. *IOP Conf Ser Mater Sci Eng*. 2018;275(1). doi:10.1088/1757-899X/275/1/012007
10. Deepa KG, Nagaraju J. Development of SnS quantum dot solar cells by SILAR method. *Mater Sci Semicond Process*. 2014;27(1):649-653. doi:10.1016/j.mssp.2014.08.006
11. Ghosh B, Das M, Banerjee P, Das S. Fabrication of SnS thin films by the successive ionic layer adsorption and reaction (SILAR) method. *Semicond Sci Technol*. 2008;23(12). doi:10.1088/0268-1242/23/12/125013

12. Suresh S, Centre CG. Wet chemical synthesis of Tin Sulfide nanoparticles and its characterization. *Int J Phys Sci*. 2014;9(17):380-385. doi:10.5897/IJPS2014.4176
13. Ravuri S, Pandey CA, Ramchandran R, Jeon SK, Grace AN. Wet Chemical Synthesis of SnS/Graphene Nanocomposites for High Performance Supercapacitor Electrodes. *Int J Nanosci*. 2018;17(1-2). doi:10.1142/S0219581X17600225
14. Vidal J, Lany S, D'Avezac M, et al. Band-structure, optical properties, and defect physics of the photovoltaic semiconductor SnS. *Appl Phys Lett*. 2012;100(3). doi:10.1063/1.3675880
15. Jain P, Arun P. Influence of grain size on the band-gap of annealed SnS thin films. *Thin Solid Films*. 2013;548:241-246. doi:10.1016/j.tsf.2013.09.089
16. Xia J, Li XZ, Huang X, et al. Physical vapor deposition synthesis of two-dimensional orthorhombic SnS flakes with strong angle/temperature-dependent Raman responses. *Nanoscale*. 2016;8(4):2063-2070. doi:10.1039/c5nr07675g
17. Kafashan H. X-ray Diffraction Line Profile Analysis of Undoped and Se-Doped SnS Thin Films Using Scherrer's, Williamson–Hall and Size–Strain Plot Methods. *J Electron Mater*. 2019;48(2):1294-1309. doi:10.1007/s11664-018-6791-7
18. Han J, Yin X, Nan H, et al. Enhancing the Performance of Perovskite Solar Cells by Hybridizing SnS Quantum Dots with CH3NH3PbI3. *Small*. 2017;13(32):1-8. doi:10.1002/smll.201700953
19. Guo W, Shen Y, Wu M, Wang L, Wang L, Ma T. SnS-quantum dot solar cells using novel TiC counter electrode and organic redox couples. *Chem - A Eur J*. 2012;18(25):7862-7868. doi:10.1002/chem.201103904
20. Li H, Ji J, Zheng X, Ma Y, Jin Z, Ji H. Preparation of SnS quantum dots for solar cells application by an in-situ solution chemical reaction process. *Mater Sci Semicond Process*. 2015;36:65-70. doi:10.1016/j.mssp.2015.03.036
21. Deepa KG, Nagaraju J. Growth and photovoltaic performance of SnS quantum dots. *Mater Sci Eng B Solid-State Mater Adv Technol*. 2012;177(13):1023-1028. doi:10.1016/j.mseb.2012.05.006
22. Rahaman S, Jagannatha KB, Pradeep, Sriram A, Anirudha, Nitin. Synthesis and Characterization of SnS Quantum Dots materialfor Solar Cell. *Mater Today Proc*. 2018;5(1):3117-3120. doi:10.1016/j.matpr.2018.01.117
23. Rana C, Bera SR, Saha S. Growth of SnS nanoparticles and its ability as ethanol gas sensor. *J Mater Sci Mater Electron*. 2019;30(3):2016-2029. doi:10.1007/s10854-018-0473-3
24. Hung NM, Nguyen C V., Arepalli VK, et al. Defect-induced gas-sensing properties of a flexible sns sensor under uv illumination at room temperature. *Sensors (Switzerland)*. 2020;20(19):1-17. doi:10.3390/s20195701
25. Nariya BB, Dasadia AK, Bhayani MK, Patel AJ, Jani AR. Electrical transport properties of SnS and SnSe single crystals grown by direct vapour transport technique. *Chalcogenide Lett*. 2009;6(10):549-554.
26. Hibbert TG, Mahon MF, Molloy KC, Price LS, Parkin IP. Deposition of tin sulfide thin films from novel, volatile (fluoroalkythiolato)tin(IV) precursors. *J Mater Chem*. 2001;11(2):469-473. doi:10.1039/b005863g
27. Kadam SR, Ghosh S, Bar-Ziv R, Bar-Sadan M. Structural Transformation of SnS2 to SnS by Mo Doping Produces Electro/Photocatalyst for Hydrogen Production. *Chem - A Eur J*. 2020;26(29):6679-6685. doi:10.1002/chem.202000366

28. Shraavya Rao, Ankithamorankar, Himanivarma, Emerging photovoltaics: organic, copper-zinc -tin sulfide and pervoskite - based solar cells,Journalof applied chemistry 2016.
29. YjYang,B.J Xiang, A simple synthesis of SnS nanoflakes at ambient conditions,Applied physics material science and processing,A.38,461-463(2006),DoI:10.1007/s00339-006-3572-6.
30. N Koteeswarareddy,M.Devika,E.S.R Gopal, Review on tin sulfide material, synthesis, properties and applications, Critical reviews in solidstate and material science 40(6), 359-398, 25 August 2015.
31. S H Chaki, Mahesh D Choudhary, M P Deshpande, J P Tailor, K S Mahatho, Synthesis and electrical transport properties of SnSnanoparticles,AIP.Conference proceedings,1512,966(2013):DOI:1000.1063/1000.4791363.
32. Hegde SS, Kunjomana AG, Ramesh K, Chandrasekharan KA, Prashantha M. Preparation and characterisation of SnS Thin Films for Solar Cell Application. *Int J Soft Comput Eng*. 2011;(July):38-40.
33. Burton LA, Colombara D, Abellon RD, et al. Synthesis, characterization, and electronic structure of single-crystal SnS, Sn2S3, and SnS2. *Chem Mater*. 2013;25(24):4908-4916. doi:10.1021/cm403046m
34. Nouman Rafiq, Waqar A.A Sayed, AuliaRifada, M.Asadghufran, Ahsan Ali, Wiqashusseinshah,Structural thermal and optical investigation of tin sulphide nanoparticles for next generation photovoltaic applications, Material science, Poland, 36 (2)2018.pp 270-275.
35. Xu Y, Al-Salim N, Bumby CW, Tilley RD. Synthesis of SnS quantum dots. *J Am Chem Soc*. 2009;131(44):15990-15991. doi:10.1021/ja906804f
36. Jitender Gour, Shilpa Jain, Suresh Chand, Narendar Kumar kaushik,Tinsulphide synthesis from waste waters, American journal of analytical chemistry,2014,5,50-54.
37. M S Omar,Solid surface and nanoscale material structure,DOI:10.13140/ROAD.2.2.3 1947.59684,Xiangtao.
38. Sohila S, Rajalakshmi M, Ghosh C, Arora AK, Muthamizhchelvan C. Optical and Raman scattering studies on SnS nanoparticles. *J Alloys Compd*. 2011;509(19):5843-5847. doi:10.1016/j.jallcom.2011.02.141
39. Sebastian S, Vinoth S, Prasad KH, et al. Quantitative analysis of Ag-doped SnS thin films for solar cell applications. *Appl Phys A Mater Sci Process*. 2020;126(10). doi:10.1007/s00339-020-03959-8
40. Mathews NR, Anaya HBM, Cortes-Jacome MA, Angeles-Chavez C, Toledo-Antonio JA. Tin Sulfide Thin Films by Pulse Electrodeposition: Structural, Morphological, and Optical Properties. *J Electrochem Soc*. 2010;157(3):H337. doi:10.1149/1.3289318
41. Chandrasekhar HR, Humphreys RG, Zwick U, Cardona M. Infrared and Raman spectra of the IV-VI compounds SnS and SnSe. *Phys Rev B*. 1977;15(4):2177-2183. doi:10.1103/PhysRevB.15.2177
42. Hidenori Noguchi, AgusSetiyadi ,HiromasaTanamura, TokaoNagatomo,Osamuomoto, Characterization of Vaccum-evaporated tin sulfide film for solar cell materials,solar energy materials and solar cells,35(1994)325-331.
43. Jakhar A, Jamdagni A, Bakshi A, et al. Refractive index of SnS thin nano-crystalline films. *Solid State Commun*. 2013;168:31-35. doi:10.1016/j.ssc.2013.06.013
44. T. S. Moss, phys. stat. sol. (b) 131 (1985) 415–427
45. Li M, Wu Y, Li T, et al. Revealing anisotropy and thickness dependence of Raman spectra for SnS flakes. *RSC Adv*. 2017;7(77):48759-48765. doi:10.1039/c7ra09430b

46. Nikolic PM, Mihajlovic P, Lavrencic B. Splitting and coupling of lattice modes in the layer compound SnS. *J Phys C Solid State Phys*. 1977;10(11). doi:10.1088/0022-3719/10/11/003
47. Choi HC, Jung YM, Kim S Bin. Size effects in the Raman spectra of TiO2 nanoparticles. *VibSpectrosc*. 2005;37(1):33-38. doi:10.1016/j.vibspec.2004.05.006
48. Li WS, Shen ZX, Li HY, Shen DZ, Fan XW. Blue shift of Raman peak from coated TiO2 nanoparticles. *J Raman Spectrosc*. 2001;32(10):862-865. doi:10.1002/jrs.773